Editors' Suggestion

Ubiquitous Superconducting Diode Effect in Superconductor Thin Films

Yasen Hou,[1,*] Fabrizio Nichele,[2] Hang Chi,[1,3] Alessandro Lodesani,[1] Yingying Wu,[1] Markus F. Ritter,[2] Daniel Z. Haxell,[2] Margarita Davydova,[4] Stefan Ilić,[5] Ourania Glezakou-Elbert,[6] Amith Varambally,[7] F. Sebastian Bergeret,[5,8] Akashdeep Kamra,[9,†] Liang Fu,[4] Patrick A. Lee,[4,‡] and Jagadeesh S. Moodera[1,4,§]

[1]*Francis Bitter Magnet Laboratory and Plasma Science and Fusion Center, Massachusetts Institute of Technology, Cambridge, Massachusetts 02139, USA*
[2]*IBM Research Europe - Zurich, Säumerstrasse 4, 8803 Rüschlikon, Switzerland*
[3]*U.S. Army DEVCOM Army Research Laboratory, Adelphi, Maryland 20783, USA*
[4]*Department of Physics, Massachusetts Institute of Technology, Cambridge, Massachusetts 02139, USA*
[5]*Centro de Física de Materiales (CFM-MPC), Centro Mixto CSIC-UPV/EHU, Pº Manuel de Lardizabal 5, Donostia-San Sebastián 20018, Spain*
[6]*Hanford High School, Richland, Washington 99354, USA*
[7]*Vestavia Hills High School, Vestavia Hills, Alabama 35216, USA*
[8]*Donostia International Physics Center (DIPC), Donostia-San Sebastián 20018, Spain*
[9]*Condensed Matter Physics Center (IFIMAC) and Departamento de Física Teórica de la Materia Condensada, Universidad Autónoma de Madrid, E-28049 Madrid, Spain*

(Received 1 November 2022; accepted 9 May 2023; published 13 July 2023)

The macroscopic coherence in superconductors supports dissipationless supercurrents that could play a central role in emerging quantum technologies. Accomplishing unequal supercurrents in the forward and backward directions would enable unprecedented functionalities. This nonreciprocity of critical supercurrents is called the superconducting (SC) diode effect. We demonstrate the strong SC diode effect in conventional SC thin films, such as niobium and vanadium, employing external magnetic fields as small as 1 Oe. Interfacing the SC layer with a ferromagnetic semiconductor EuS, we further accomplish the nonvolatile SC diode effect reaching a giant efficiency of 65%. By careful control experiments and theoretical modeling, we demonstrate that the critical supercurrent nonreciprocity in SC thin films could be easily accomplished with asymmetrical vortex edge and surface barriers and the universal Meissner screening current governing the critical currents. Our engineering of the SC diode effect in simple systems opens the door for novel technologies while revealing the ubiquity of the Meissner screening effect induced SC diode effect in superconducting films, and it should be eliminated with great care in the search for exotic superconducting states harboring finite-momentum Cooper pairing.

DOI: 10.1103/PhysRevLett.131.027001

Introduction.—Similar to a conventional semiconductor diode, a superconductor with nonreciprocal current flow, a superconducting (SC) diode, may form building blocks for, e.g., dissipationless SC digital logic. The recent observation of such a SC diode effect in a complex thin film superconductor heterostructure subjected to an external magnetic field has stimulated vigorous activity towards understanding and replicating it [1]. Supercurrent rectification has also been demonstrated in multiple Josephson junction systems including Al-InGaAs/InAs-Al [2], $NbSe_2/Nb_3Br_8/NbSe_2$ [3] and Nb-$NiTe_2$-Nb [4], where the largest nonreciprocities are observed at large in-plane magnetic fields [2,4]. Furthermore, an intrinsic SC diode effect has been observed in few-layer $NbSe_2$ [5] and twisted trilayer graphene/WTe_2 heterostructures [6] in an out-of-plane magnetic field. To quantify the diode effect, it is common to introduce an asymmetry parameter, called the diode efficiency $\eta = [(I_c^+ - I_c^-)/(I_c^+ + I_c^-)]$, where I_c^+ and I_c^- are the critical currents in the two opposite directions. The value of η denotes the magnitude of the diode effect, while the sign defines the polarity. Up to now, reported values of η range from a few percent to 30% [1–6].

Several theoretical mechanisms have been proposed to explain the SC diode effects in superconductors [7–11] and in Josephson junctions [12,13], with special emphasis on the potential role of the finite-momentum Cooper pairing [7–13]. While this mechanism focuses on the intrinsic depairing current [7–13], it is known that nearly all the superconductor films fail to be governed by the critical pair breaking mechanism, which merely offers the theoretical maximum for a specially designed sample [14–16]. A broad range of

other mechanisms come to govern different samples [17,18]. Magnetic flux, or Abrikosov vortices, are normally pinned to defect centers or surfaces of a superconductor [19]. The current flow, however, produces a Lorentz force on the vortices. A critical current is often measured when the pinning centers or the surface barrier cannot hold vortices anymore and dissipation starts in the superconductor [18,20–22]. This principle has been exploited to engineer superconducting vortices-based rectifiers [23–27]. Furthermore, Vodolazov and Peeters predicted existence and engineering of SC diode effect employing controlled edge disorder [23]. This escaped experimental realization thus far and the present work accomplishes it.

Here, using V and Nb superconductors, three types of the SC diode effect are demonstrated, two of which are rooted in the universal Meissner screening instead of the rare finite-momentum Cooper pairing. We show a robust control of the nonreciprocity with record high efficiency in conventional superconductors without requiring additional spin-orbit coupling (SOC) and/or exchange fields.

Results.—The V, Nb, and EuS films in our experiments were deposited on clean, heated sapphire substrates in a single deposition process in a molecular-beam epitaxy chamber (base pressure $<4\times10^{-10}$ Torr) [28]. The thicknesses (d_m, d) of EuS and V (or Nb) were, respectively, 5 and 8 nm. The film was patterned by e-beam lithography and Ar ion milling into a Hall bar geometry, with width $W\sim8$ μm and length $L\sim48$ μm [Fig. 1(a)]. The patterned V device had T_c of 3.5 K–4.3 K and a residual resistance ratio around 3 (Supplemental Material [29]). Four-probe geometry current vs voltage scans were measured to observe the critical current (I_c) nonreciprocity. The I-V scans taken at 1.8 K for a V film subjected to out-of-plane magnetic field are shown in Fig. 1(b). Increasing and decreasing current sweeps showed distinctly different I_c values: $I_c^{\pm}$ marking the SC to normal state transition, whereas a much smaller retrapping current $I_r^{\pm}$ was recorded while transitioning back from the normal to the SC state [Fig. 1(b)]. The low $I_r^{\pm}$ is often attributed to self-heating when the film is in the normal state [3,4]. In this study, we focus on $I_c^{\pm}$, where the nonreciprocity was controllable by applying an out-of-plane magnetic field. With the 2.8 Oe field applied along the $+z$ direction, I_c for positive direction (I_c^+) was significantly larger than when the current flow was in the negative direction (I_c^-). By reversing the magnetic field the I_c^+ and I_c^- magnitudes interchanged. The magnetic field dependence of I_c^+ and I_c^- is plotted in Fig. 1(c); I_c showing large field dependence, an "inverted V" shape, with peaks occurring at ±2.5 Oe. A noticeable current rectification occurred even for fields <1 Oe, with its polarity controllable by the field direction. The diode efficiency versus magnetic field in Fig. 1(c) exhibits a maximum efficiency of ∼19% at ±2.8 Oe. Such supercurrent rectification (type A) was observed in all the superconducting devices that we measured. I-V scans of another V device

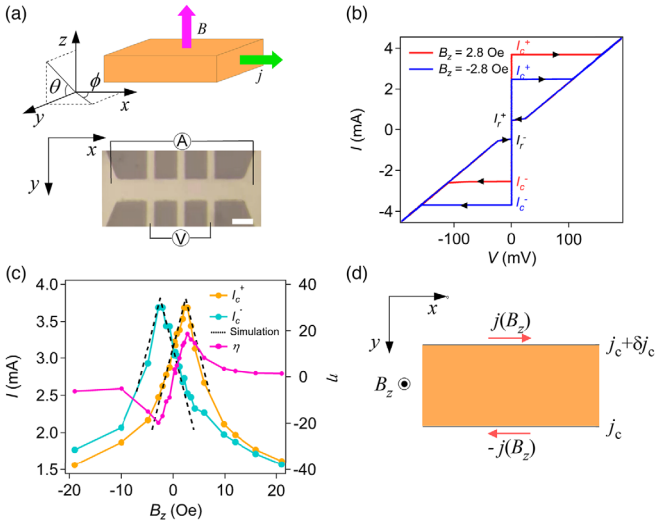

FIG. 1. Demonstration of out-of-plane field induced diode effect in a SC film at 1.8 K. (a) Top: schematic drawing of the vanadium thin film strip. Bottom: optical microscope image of the Hall bar strip of V film. Scale bar denotes 8 μm. (b) I-V scans of the device at 2.8 Oe out-of-plane field along $\pm z$ direction as indicated by the red and blue lines. Black arrows indicate the scan direction. (c) Critical currents and diode efficiency as a function of the magnetic field. Black dashed lines show the calculated critical current values based on our model. (d) Schematic depiction of Meissner screening currents and the asymmetry between the critical current densities at the two edges.

and a Nb device are presented in the Supplemental Material [29], showing similar I_c nonreciprocity for an out-of-plane magnetic field.

For the current flow in a superconductor without breaking the mirror symmetry with respect to the x-z plane, the $+x$ and $-x$ directions are equivalent. Thus, we attribute the observed diode effect to a combination of Meissner current generated to screen the applied magnetic field and symmetry breaking of the device edges during fabrication. In practice, the two edges of a SC stripe could never be identical, thereby admitting slightly different critical current densities j_c and $j_c+\delta j_c$, which are smaller than the Ginzburg-Landau depairing limit j_{GL}, as indicated in Fig. 1(d). When current density in the device is above j_c, the Lorentz force on vortices nucleated at the edge overcomes the Bean-Livingston barrier thereby enabling vortex flow through the sample which destroys superconductivity [20,23,31–33]. The Meissner effect induces two dissipationless counterflowing screening current densities $\pm j(B_z)$ at the two edges, when an out-of-plane field is applied. This screening current adds or subtracts to the applied current at opposite edges, and modifies the measured values of j_c^+ and j_c^-. At small fields, the screening current density is simply the Meissner response $j(B_z)=aB_z$, linear with the applied magnetic field, where a is a constant. The current flowing along top or bottom edge is the net current, which is applied current $(j_{\mathrm{ext}})+/-$ Meissner screening current

$[j(B_z)]$. For the case shown in Fig. 1(d), on the $B_z > 0$ side (see Supplemental Material [29] for a detailed derivation),

$$j_c^+ = j_c + aB_z, \qquad j_c^- = j_c - aB_z, \quad \text{when } aB_z < \frac{\delta j_c}{2}, \tag{1}$$

$$j_c^+ = j_c + \delta j_c - aB_z, \qquad j_c^- = j_c - aB_z, \quad \text{when } aB_z \geq \frac{\delta j_c}{2}. \tag{2}$$

Similar results are obtained for reversed field. Assuming a uniform current flow in the superconducting stripe, we have $I_c^\pm = Sj_c^\pm$, where S is the device cross section.

$$I_c^+ = S(j_c + aB_z), \qquad I_c^- = S(j_c - aB_z), \quad \text{when } aB_z < \frac{\delta j_c}{2}, \tag{3}$$

$$I_c^+ = S(j_c + \delta j_c - aB_z), \qquad I_c^- = S(j_c - aB_z), \quad \text{when } aB_z \geq \frac{\delta j_c}{2}. \tag{4}$$

The experimental data could be fitted with $Sj_c = 3.14$ mA, $S\delta j_c = 1.35$ mA, and $Sa = 0.275$ mA.Oe^{-1} as shown by the dashed curves in Fig. 1(c). Such a drastic suppression of I_c by out-of-plane magnetic field in the thin film geometry could be understood by the ineffective Meissner screening [34,35] as is detailed in the Supplemental Material [29]. As the field increases, a sublinear dependence of I_c on B is observed, due to the transition from surface pinning to bulk pinning determining I_c (Supplemental Material [29]).

As the peak diode efficiency is determined by the edge asymmetry, we fabricated devices with and without a lithographically defined edge asymmetry (serrated edge with a lateral size of 3 μm, much larger than the coherence length) [36]. Critical current vs magnetic field for both devices are shown in the Supplemental Material [29]. The device without defined asymmetry shows a peak value for diode efficiency of 21%, while the one with a serrated edge attains a much larger diode efficiency, reaching ∼50%. Critical current peaks of the device with defined asymmetry occur at ±5.1 Oe, larger than 1.5 Oe for the device without it, which shows (and agrees with) a lower critical current for the serrated edges [36]. As the temperature increases, both critical currents and diode efficiency drop as detailed in the Supplemental Material [29]. The main reason behind such a strong effect of the etching inhomogeneities is that the critical current in the devices is being determined by (i) vortex surface barrier, which is highly sensitive to the superconductor quality at the edges, and (ii) the current density at the edges. As per the contribution of (i) above, a deterioration in the superconducting properties close to an edge due to the etching-related disorder may lead to a significant lowering of the vortex surface barrier. As per the contribution (ii) listed above, the current density at the edge may be locally enhanced due to disorder for the a given total current through the superconductor [36]. These results further support the Meissner screening and asymmetric vortex surface barriers to be the underlying mechanism and a practical approach to enhance the diode efficiency [23].

Because of the highly sensitive dependence of I_c on the out-of-plane field, a false "in-plane" magnetic field induced diode effect could easily be measured, with an offset between the magnetic field direction and the film plane by as small as 0.01° (Supplemental Material [29]). Hence, while investigating the SC diode effect under an in-plane magnetic field, any out-of-plane component of the field needs to be carefully removed to interpret the data. To study the effects of the real in-plane magnetic field on the critical currents, we developed a technique that enabled us to remove the out-of-plane field up to an accuracy of <0.1 Oe (Supplemental Material [29]). A diode effect (type B) is then observed when the in-plane magnetic field is both parallel and perpendicular to the current flow (Supplemental Material [29]). The physical origin for this type of diode effect remains unclear and encourages further exploration—theoretical and experimental.

Experimentally, a drastic suppression of I_c by an out-of-plane field has been reported in other superconductor films such as NbN [37], TaN [37], MgB_2 [38], (Li,Fe)OHFeSe [39], and $Nb/SrRuO_3$ bilayers [40]. However, no asymmetrical I_c were reported except for an earlier work on grainy Sn films which was largely unnoticed by the community [41].

We investigated furthermore the I_c rectification of the third kind (type C) in a hybrid structure where the SC film has a ferromagnetic layer EuS over it. A 5 nm thick EuS film shows a Curie temperature comparable to the bulk value and the hysteresis loop of EuS at 1.8 K shows nice rectangular shape (Supplemental Material [29]). Figure 2(a) shows the I-V scans of a Pt/V/EuS trilayer when the EuS layer was magnetized along the y direction (in-plane and perpendicular to the current flow). 0.2 nm of Pt is deposited to provide spin-orbit coupling and Rashba splitting at the V surface [42,43]. With a small external field to magnetize the EuS layer, a dramatic difference was observed between I_c along the positive and negative directions of current flow. At $B_y = -30$ Oe, I_c^+ was more than 4 times larger than I_c^-, producing a giant I_c ratio of 480% and a diode efficiency of 65%, the highest value of diode rectification seen in superconductors yet. The I_c asymmetry was reversed when the EuS magnetization direction was flipped. The temperature, magnetic field, and angle dependencies of the SC diode effect were systematically studied on a second Pt/V/EuS device. A clear supercurrent rectification is also demonstrated in Supplemental Material [29]. As the temperature increased, I_c^+ and I_c^- reduced whereas η remained nearly unchanged

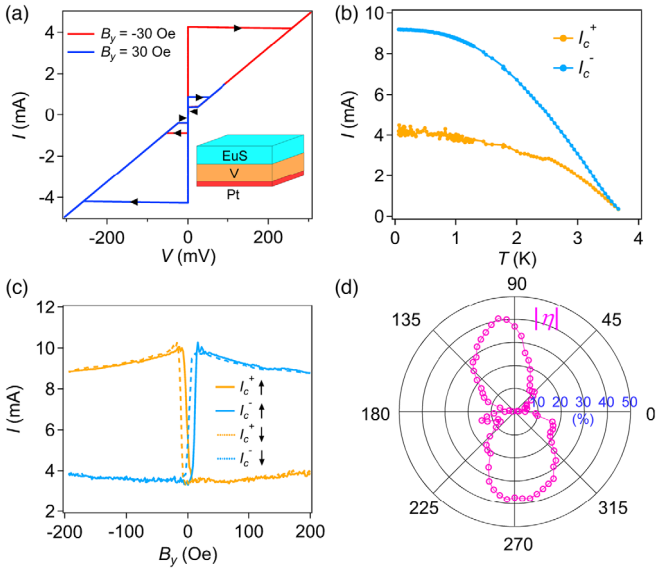

FIG. 2. SC diode effect in Pt/V/EuS trilayers. (a) I-V scans of a Pt/V/EuS device showing giant critical current rectification effect at 1.8 K. Inset shows a schematic of the Pt/V/EuS stack. (b) Temperature dependence of the critical current at $B_y = 200$ Oe. (c) Magnetic field dependence of the critical current at 1 K. Solid (dashed) lines were obtained when scanning the magnetic field up (down). (d) Angle (ϕ) dependence of η at $T = 1$ K and $B = 200$ Oe. Data in (a) and (b)–(d) are from two different Pt/V/EuS devices.

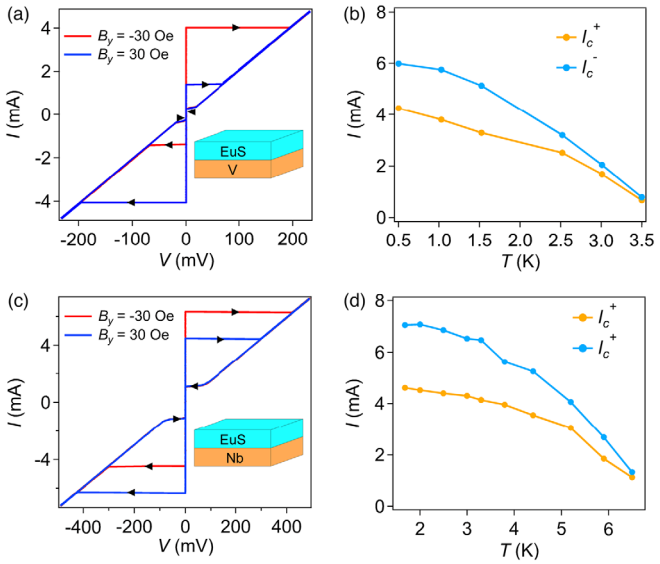

FIG. 3. SC diode effect in SC/FM bilayers. (a) I-V scans of a V/EuS device showing a similarly large SC diode effect as in Pt/V/EuS. Inset shows a schematic of the V/EuS stack. (b) Temperature dependence of the critical currents for a second V/EuS at $B_y = 30$ Oe. (c) I-V scans of a Nb/EuS device exhibiting nonreciprocity. Inset shows a schematic of the Nb/EuS stack. (d) Temperature dependence of the critical currents at $B_y = 30$ Oe for the same Nb/EuS device.

from 60 mK up to 1.3 K [Fig. 2(b)]. Further increase of the temperature led to a decrease of I_c^+, I_c^-, and η, although a clear diode phenomenon was seen even up to 3.6 K, close to T_c. At 1 K, the effect was found to quickly reach a maximum value as the field was increased to 18 Oe [Fig. 2(c)], and beyond that I_c^+, I_c^-, and η decreased slightly as the field increased. Hysteresis in I_c and η diode efficiency was observed which resembled the magnetic hysteresis of the EuS film. This hysteresis in I_c enables control of the diode polarity via the remnant EuS magnetization direction, for field-free scenario. Diode efficiency at zero external field, though a little smaller than the maximum value when EuS is fully magnetized, was still 21% for the Pt/V/EuS device. Figure 2(d) shows η on a polar plot: the largest asymmetry was for the magnetic field perpendicular to the current flow direction, while it was negligible when the field was parallel to the current flow.

It is tempting to interpret the giant supercurrent rectification in Pt/V/EuS as support for the finite-momentum pairing mechanism with Pt providing the required Rashba SOC [42,43] and exchange coupling with EuS giving a large spin-splitting in the V layer [44]. However, upon further investigations, we discovered that a similarly large nonreciprocity could be observed in a V/EuS bilayer device, without Pt providing the Rashba SOC [Fig. 3(a)]. Temperature [Fig. 3(b)], magnetic field, and angle (Supplemental Material [29]) dependencies of the SC diode effect were systematically measured on a second V/EuS device, all showing close resemblance to that of Pt/V/EuS. Moreover, Figs. 3(c)–3(d) show a similar EuS-magnetization-controlled diode effect in Nb/EuS bilayers, and persisting up to 6.5 K, as the T_c for Nb was higher than V [Fig. 4(a)].

To further examine the role of the exchange field, Nb/EuS and Nb/Al_2O_3/EuS films were grown in one deposition cycle, and a mask was used to cover one of them during the 3 nm-thick Al_2O_3 film spacer layer deposition. I-V scans at 1.8 K showed that both samples had very similar I_c when EuS was magnetized [Figs. 4(b)–4(c)]; I_c nonreciprocity in Nb/Al_2O_3/EuS trilayer, comparable to Nb/EuS bilayer. This shows that a direct contact between the SC and FM layer was not required for the type C diode effect. Based on these observations, we conclude that neither Rashba SOC nor interfacial exchange with the FM are essential in the observed I_c nonreciprocity.

The diode effect in SC/FM bilayers has been reported in other systems [32,45–49]. The phenomenon could be understood by a screening current mechanism [32] shown schematically in Fig. 4(d). The in-plane magnetization along the y axis of the FM layer produces oppositely oriented fringing fields in the y-z plane at the two edges. A calculation shows that, for distances $r > d_m$, the fringing field can be viewed as emerging radially from point sources with opposite signs at the opposite edges and decaying as

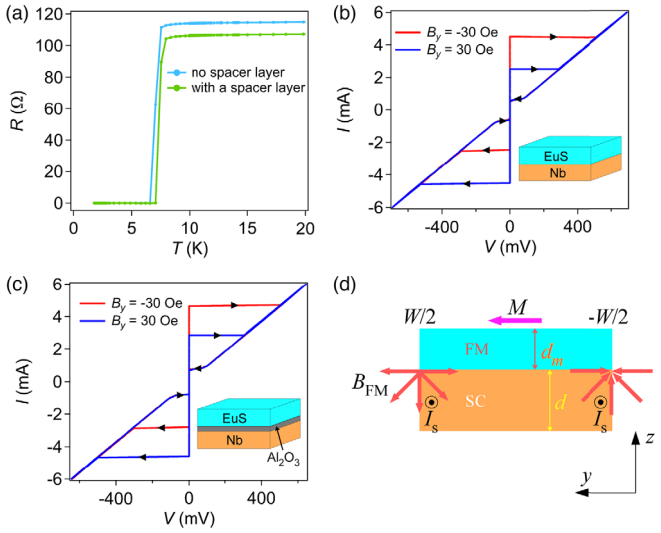

FIG. 4. (a) Resistance vs temperature shows the superconducting transition for Nb film in SC/FM bilayer with and without a 3 nm Al_2O_3 spacer layer. (b) I-V scans of the Nb/EuS device measured at 1.8 K showing type C SC diode effects. Inset shows the schematic of Nb/EuS stack. (c) I-V scans of the $Nb/Al_2O_3/EuS$ device at 1.8 K showing similar diode effects as in (b). Inset shows the $Nb/Al_2O_3/EuS$ stack structure. (d) Screening current mechanism for the SC diode effect in SC/FM bilayers. Schematic of the screening currents (IS) induced by the out-of-plane edge magnetic fields due to the EuS layer.

$1/r$ [50]. This produces a z component of the magnetic field,

$$B_z = 2md_m z/(z^2 + y^2), \tag{5}$$

where z and y are measured from the sample edges and m is the magnetization density. For EuS, the Eu moment is $\mu_s = 7\mu_B$ and estimate $4\pi m \sim 1.5$ T [51,52]. Similar to the type A, this perpendicular magnetic field produces a Meissner screening current flowing in the $+x$ direction, with two important differences. Since the fringing field reverses direction on the two edges, the screening current on both edges flows in the same direction [Fig. 4(d)], and a diode effect occurs without requiring edge asymmetry as in type A and the sign is independent of the material combination. This current adds to the external current in the $+x$ direction, but partly cancels it in $-x$ direction, resulting in a smaller I_c^+ and larger I_c^-. By reversing EuS magnetization, screening current around the edges flows along $-x$ direction, which reverses the current asymmetry. A second difference is that, unlike a uniform applied magnetic field, the fringing fields are strongly localized near the edges. Per our estimation (Supplemental Material [29]), the magnitude of the screening current is comparable to the depairing current, leading to a gigantic diode effect.

In summary, we demonstrated a ubiquitous superconducting diode effect in thin film superconductors without the need for spin-orbit or direct exchange coupling, and thus without having to invoke an exotic superconducting state harboring finite-momentum pairing. Our Letter shows that vortex surface barriers, and not pair breaking, determine the critical currents in two-dimensional or thin film superconductors. Hence, studying a potential finite-momentum paired superconducting order in a film using critical current nonreciprocity can only be accomplished via a careful device design that eliminates the role of vortices in determining the critical current, and as a result achieves the pair breaking mechanism. Consequently, recent reports treating the SC diode effect as a proof of finite-momentum pairing need to be reconsidered. From prospective technology development, we demonstrated a giant diode efficiency of 21% (65%) using no (small 30 Oe) external magnetic field for a nonvolatile diode effect, setting the stage for envisioning computation architectures based on superconducting rectification and providing a fresh impetus to the ongoing development of superconductors-based quantum technologies.

The data that support the findings of this study are available from the corresponding authors upon request. This work was supported by Air Force Office of Sponsored Research (FA9550-23-1-0004 DEF), Office of Naval Research (N00014-20-1-2306), National Science Foundation (NSF-DMR 1700137, 2218550 and 1231319); Army Research Office (W911NF-20-2-0061, DURIP W911NF-20-1-0074). F. N., M. F. R., and D. Z. H. acknowledge support from the European Research Council (Grant No. 804273). H. C. is sponsored by the Army Research Laboratory under Cooperative Agreement Number W911NF-19-2-0015. S. I. and F. S. B. are supported by European Union's Horizon 2020 Research and Innovation Framework Programme under Grant No. 800923 (SUPERTED), and the Spanish Ministerio de Ciencia e Innovacion (MICINN) through Project PID2020–114252 GBI00 (SPIRIT). F. S. B. acknowledges financial support by the A.v. Humboldt Foundation. A. K. acknowledges the support by the Spanish Ministry for Science and Innovation—AEI Grant CEX2018-000805-M (through the "Maria de Maeztu" Programme for Units of Excellence in R&D, and Grant RYC2021-031063-I.). P. A. L. acknowledges the support by DOE office of Basic Sciences Grant No. DE-FG0203ER46076. Y. H., J. S. M., L. F., F. S. B., and P. A. L. conceived and designed the study. Y. H. grew the samples and fabricated the devices. Y. H. and F. N. performed the measurements. H. C., A. L., Y. W., M. F. R., and D. Z. H. assisted with the measurements. O. G. E. and A. V. fabricated devices with defined edges and performed measurements on the devices. Y. H., A. K., P. A. L., and J. S. M. performed theory modeling. M. D., S. I., F. S. B., and L. F. provided discussion and theoretical support. Y. H., A. K., P. A. L., and J. S. M. wrote the Letter with contributions from all authors. The authors declare no competing interests.

*Corresponding author.
yshou@mit.edu
†Corresponding author.
akashdeep.kamra@uam.es
‡Corresponding author.
palee@mit.edu
§Corresponding author.
moodera@mit.edu

[1] F. Ando, Y. Miyasaka, T. Li, J. Ishizuka, T. Arakawa, Y. Shiota, T. Moriyama, Y. Yanase, and T. Ono, Nature (London) **584**, 373 (2020).
[2] C. Baumgartner *et al.*, Nat. Nanotechnol. **17**, 39 (2022).
[3] H. Wu, Y. Wang, Y. Xu, P. K. Sivakumar, C. Pasco, U. Filippozzi, S. S. P. Parkin, Y.-J. Zeng, T. McQueen, and M. N. Ali, Nature (London) **604**, 653 (2022).
[4] B. Pal *et al.*, Nat. Phys. **18**, 1228 (2022).
[5] L. Bauriedl *et al.*, Nat. Commun. **13**, 4266 (2022).
[6] J.-X. Lin, P. Siriviboon, H. D. Scammell, S. Liu, D. Rhodes, K. Watanabe, T. Taniguchi, J. Hone, M. S. Scheurer, and J. I. A. Li, Nat. Phys. **18**, 1221 (2022).
[7] A. Daido, Y. Ikeda, and Y. Yanase, Phys. Rev. Lett. **128**, 037001 (2022).
[8] S. Ilić and F. S. Bergeret, Phys. Rev. Lett. **128**, 177001 (2022).
[9] N. F. Q. Yuan and L. Fu, Proc. Natl. Acad. Sci. U.S.A. **119**, e2119548119 (2022).
[10] J. J. He, Y. Tanaka, and N. Nagaosa, New J. Phys. **24**, 053014 (2022).
[11] H. D. Scammell, J. I. A. Li, and M. S. Scheurer, 2D Mater. **9**, 025027 (2022).
[12] M. Davydova, S. Prembabu, and L. Fu, Sci. Adv. **8**, eabo0309 (2022).
[13] Y. Tanaka, B. Lu, and N. Nagaosa, Phys. Rev. B **106**, 214524 (2022).
[14] K. Xu, P. Cao, and J. R. Heath, Nano Lett. **10**, 4206 (2010).
[15] C. P. Poole, *Handbook of Superconductivity* (Academic Press, San Diego, 2000).
[16] C. C. Tsuei, J. Mannhart, and D. Dimos, AIP Conf. Proc. **182**, 194 (1989).
[17] K. K. Likharev, Rev. Mod. Phys. **51**, 101 (1979).
[18] V. V. Shmidt, Sov. Phys. Usp. **13**, 408 (1970).
[19] C. P. Bean and J. D. Livingston, Phys. Rev. Lett. **12**, 14 (1964).
[20] V. V. Shmidt, Sov. Phy. JETP **30**, 1137 (1970).
[21] M. K. Hope, M. Amundsen, D. Suri, J. S. Moodera, and A. Kamra, Phys. Rev. B **104**, 184512 (2021).
[22] A. Buzdin and M. Daumens, Physica (Amsterdam) **294C**, 257 (1998).
[23] D. Y. Vodolazov and F. M. Peeters, Phys. Rev. B **72**, 172508 (2005).
[24] C. S. Lee, B. Jankó, I. Derényi, and A. L. Barabási, Nature (London) **400**, 337 (1999).
[25] J. E. Villegas, S. Savel'ev, F. Nori, E. M. Gonzalez, J. V. Anguita, R. García, and J. L. Vicent, Science **302**, 1188 (2003).
[26] J. E. Villegas, E. M. Gonzalez, M. P. Gonzalez, J. V. Anguita, and J. L. Vicent, Phys. Rev. B **71**, 024519 (2005).
[27] D. Cerbu, V. N. Gladilin, J. Cuppens, J. Fritzsche, J. Tempere, J. T. Devreese, V. V. Moshchalkov, A. V. Silhanek, and J. Van de Vondel, New J. Phys. **15**, 063022 (2013).
[28] P. Wei, F. Katmis, C.-Z. Chang, and J. S. Moodera, Nano Lett. **16**, 2714 (2016).
[29] See Supplemental Material at http://link.aps.org/supplemental/10.1103/PhysRevLett.131.027001 for additional details on experiments and theory, which includes Ref. [30].
[30] N. R. Werthamer, E. Helfand, and P. C. Hohenberg, Phys. Rev. **147**, 295 (1966).
[31] M. Benkraouda and J. R. Clem, Phys. Rev. B **58**, 15103 (1998).
[32] D. Y. Vodolazov, B. A. Gribkov, S. A. Gusev, A. Y. Klimov, Y. N. Nozdrin, V. V. Rogov, and S. N. Vdovichev, Phys. Rev. B **72**, 064509 (2005).
[33] M. Kupriyanov and K. Likharev, Sov. Phys. Solid State **16**, 1835 (1975), https://www.osti.gov/biblio/4222593.
[34] G. M. Maksimova, Phys. Solid State **40**, 1607 (1998).
[35] J. Pearl, Appl. Phys. Lett. **5**, 65 (1964).
[36] J. R. Clem and K. K. Berggren, Phys. Rev. B **84**, 174510 (2011).
[37] K. Ilin, D. Henrich, Y. Luck, Y. Liang, M. Siegel, and D. Y. Vodolazov, Phys. Rev. B **89**, 184511 (2014).
[38] C. B. Eom *et al.*, Nature (London) **411**, 558 (2001).
[39] J. Hänisch, Y. Huang, D. Li, J. Yuan, K. Jin, X. Dong, E. Talantsev, B. Holzapfel, and Z. Zhao, Supercond. Sci. Technol. **33**, 114009 (2020).
[40] M. Feigenson, L. Klein, M. Karpovski, J. W. Reiner, and M. R. Beasley, J. Appl. Phys. **97**, 10J120 (2005).
[41] A. G. Sivakov, O. G. Turutanov, A. E. Kolinko, and A. S. Pokhila, Low Temp. Phys. **44**, 226 (2018).
[42] R. Meservey and P. M. Tedrow, Phys. Rep. **238**, 173 (1994).
[43] P. Fulde, Adv. Phys. **22**, 667 (1973).
[44] P. Wei, F. Katmis, B. A. Assaf, H. Steinberg, P. Jarillo-Herrero, D. Heiman, and J. S. Moodera, Phys. Rev. Lett. **110**, 186807 (2013).
[45] M. V. Milošević, G. R. Berdiyorov, and F. M. Peeters, Phys. Rev. Lett. **95**, 147004 (2005).
[46] N. Touitou, P. Bernstein, J. F. Hamet, C. Simon, L. Méchin, J. P. Contour, and E. Jacquet, Appl. Phys. Lett. **85**, 1742 (2004).
[47] A. Papon, K. Senapati, and Z. H. Barber, Appl. Phys. Lett. **93**, 172507 (2008).
[48] G. Carapella, P. Sabatino, and G. Costabile, Phys. Rev. B **81**, 054503 (2010).
[49] G. Carapella, V. Granata, F. Russo, and G. Costabile, Appl. Phys. Lett. **94**, 242504 (2009).
[50] Y. Liu *et al.*, Nano Lett. **20**, 456 (2020).
[51] A. Svane, G. Santi, Z. Szotek, W. M. Temmerman, P. Strange, M. Horne, G. Vaitheeswaran, V. Kanchana, L. Petit, and H. Winter, Phys. Status Solidi (b) **241**, 3185 (2004).
[52] A. Mauger and C. Godart, Phys. Rep. **141**, 51 (1986).